



Physical controls on the storage of methane in landfast sea ice

J. Zhou^{1,2}, J.-L. Tison¹, G. Carnat¹, N.-X. Geilfus³, and B. Delille²

¹Laboratoire de glaciologie, DSTE, Université Libre de Bruxelles, Brussels, Belgium

²Unité d'Océanographie chimique, MARE, Université de Liège, Liège, Belgium

³Arctic Research Center, Aarhus University, Aarhus, Denmark

Correspondence to: J. Zhou (jiayzhou@ulb.ac.be)

Received: 13 November 2013 – Published in The Cryosphere Discuss.: 6 January 2014

Revised: 17 April 2014 – Accepted: 22 April 2014 – Published: 3 June 2014

Abstract. We report on methane (CH₄) dynamics in landfast sea ice, brine and under-ice seawater at Barrow in 2009. The CH₄ concentrations in under-ice water ranged from 25.9 to 116.4 nmol L_{sw}⁻¹, indicating a supersaturation of 700 to 3100 % relative to the atmosphere. In comparison, the CH₄ concentrations in sea ice ranged from 3.4 to 17.2 nmol L_{ice}⁻¹ and the deduced CH₄ concentrations in brine from 13.2 to 677.7 nmol L_{brine}⁻¹. We investigated the processes underlying the difference in CH₄ concentrations between sea ice, brine and under-ice water and suggest that biological controls on the storage of CH₄ in ice were minor in comparison to the physical controls. Two physical processes regulated the storage of CH₄ in our landfast ice samples: bubble formation within the ice and sea ice permeability. Gas bubble formation due to brine concentration and solubility decrease favoured the accumulation of CH₄ in the ice at the beginning of ice growth. CH₄ retention in sea ice was then twice as efficient as that of salt; this also explains the overall higher CH₄ concentrations in brine than in the under-ice water. As sea ice thickened, gas bubble formation became less efficient, CH₄ was then mainly trapped in the dissolved state. The increase of sea ice permeability during ice melt marked the end of CH₄ storage.

radiative forcing of well-mixed greenhouse gases (Myhre et al., 2013).

Global ocean emission of CH₄ is estimated at 19 Tg per year (Kirschke et al., 2013), which is about 3 % of the global tropospheric CH₄ input. Of that marine contribution, 75 % is from coastal regions (Bange et al., 1994). CH₄ supersaturation relative to the atmosphere in estuaries (Borges and Abril, 2011; Upstill-Goddard et al., 2000) and coastal shelves (Kvenvolden et al., 1993; Savvichev et al., 2004; Shakhova et al., 2005, 2010) is indeed larger than that in the open ocean (Bates et al., 1996; Damm et al., 2007, 2008, 2010).

Methanogenesis in submarine sediments is thought to be the main process causing CH₄ efflux in the Arctic shelf regions. Nonetheless, other sources could also be significant: CH₄ seepage from coastal ice-complex deposits (Romanovskii et al., 2000) and from deeper seabeds (Judd, 2004), and CH₄ dissociation in the shallow hydrates (Reagan and Moridis, 2008; Westbrook et al., 2009). Recently, aerobic CH₄ production in the water column related to dimethylsulfoniopropionate (DMSP) degradation was reported for the central Arctic (Damm et al., 2010), tropical upwelling areas (Florez-Leiva et al., 2013) and tropical oligotrophic areas (Zindler et al., 2013). However, the significance of that process over the Arctic shelf still needs to be assessed.

Ongoing global warming is likely to affect the various sources of CH₄ cited above, with positive feedback on the climate. Indeed, a rise in sea temperature should increase methanogenic activities, leading to a more efficient conversion of organic matter to CH₄ (Zeikus and Winfrey, 1976). In addition, the induced seawater stratification is likely to change the nutrient ratio, which favours aerobic CH₄ production (Karl et al., 2008). Moreover, warmer seawater is likely to weaken the coastal ice complex (including subsea

1 Introduction

Methane (CH₄) is a well-mixed greenhouse gas. Its concentration in the atmosphere is much lower than that of its oxidation product (CO₂) (1.9 vs. 397 ppm respectively) (<http://www.esrl.noaa.gov/gmd/aggi/>). However, since the CH₄ global warming potential is 28 times higher than that of CO₂ over a 100-year frame, it accounts for 20 % of the global

permafrost) (Lawrence et al., 2008) and to displace the gas hydrate stability zones (Reagan and Moridis, 2008), increasing gas seepage. Significant CH₄ escape has recently been detected via acoustic surveys along the Spitsbergen continental margin (Westbrook et al., 2009), suggesting that changes in the CH₄ storage system are ongoing. Since CH₄ has a high global warming potential, its release will enhance global warming, which in turn will enhance methanogenic activities and gas seepages. This positive feedback has contributed to rapid and significant climate warming in the past (O'Connor et al., 2010).

Understanding the current CH₄ budget is thus important in order to better simulate future climate scenarios. Many CH₄ measurements have been carried out in sediments and seawater throughout the coastal Arctic areas (Kvenvolden et al., 1993; Savvichev et al., 2004; Shakhova et al., 2005, 2010). These observations have led to speculations about potential CH₄ accumulation (Shakhova et al., 2010) and/or oxidation (Kitidis et al., 2010) under sea ice cover. Other studies further brought forward the role of sea ice in the exchange of CH₄ between seawater and the atmosphere (He et al., 2013; Kort et al., 2012). However, to the best of our knowledge, no study has yet discussed the physical controls on the storage of CH₄ in sea ice and its exchange at the atmosphere–ice–ocean interfaces. For instance, CH₄ mixing ratios up to 11 000 ppmV have been measured in sea ice bubbles (Shakhova et al., 2010), but the mechanisms leading to the incorporation of those gas bubbles within the ice have not been discussed. Similarly, He et al. (2013) suggested CH₄ consumption in the ice, based on CH₄ fluxes above sea ice. However, they did not discuss the impact of sea ice permeability or ice melt on their results, although these parameters have been shown to affect other gas dynamics in sea ice (see, e.g., Loose et al. (2009) for O₂ and SF₆, Geilfus et al. (2012) and Nomura et al. (2010) for CO₂, and Zhou et al. (2013) for Ar). Therefore, we felt it necessary to highlight the physical controls on CH₄ dynamics in sea ice, from ice growth to ice melt. We have done this by investigating the annual evolution of CH₄ concentrations in sea ice, in parallel with sea ice physical properties, and CH₄ concentrations in seawater. To the best of our knowledge, we report here the first detailed time series of CH₄ concentrations in sea ice across seasons.

2 Materials and methods

2.1 Study site and physical framework

Sea ice and under-ice seawater samples were collected during a field survey in the Chukchi Sea near Barrow (Alaska) (Fig. 1) from January through June 2009. The sampling was performed on level first-year landfast sea ice, within a square of 50 m by 50 m. The north-eastern corner of the square was located at 71°22.013' N, 156°32.447' W. Seawater depth at the location was about 6.5 m (<http://seaice.alaska.edu/gi/>

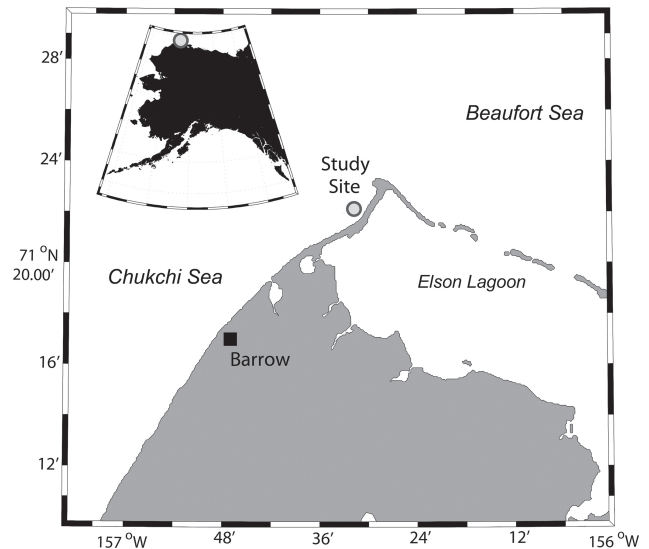


Figure 1. The study site (north of Barrow, Alaska, USA).

observatories/barrow_sealevel). Ice cores were extracted and kept in darkness in the laboratory at -35°C to prevent brine drainage and to limit biological activity. Temperature recorders indicated that the samples were always kept below -20°C during transport. All of the analyses were completed within the following year. A complete physical framework of the present study is presented and discussed in Zhou et al. (2013). We have selected six sampling events to illustrate the evolution of CH₄ concentrations at our location: one in the winter (BRW2; 3 February), four in early spring (BRW4, BRW5, BRW6 and BRW7; corresponding to 31 March, 3, 7 and 10 April respectively), and the final one in late spring (BRW10; 5 June). The first five sampling events occurred during ice growth, the last one during ice decay.

2.2 CH₄ concentrations in seawater

CH₄ concentrations in seawater were determined by gas chromatography (GC) with flame ionization detection (SRI 8610C GC-FID) (Skoog et al., 1997) after creating a 30 mL headspace with N₂ in 70 mL glass serum bottles, following the procedure described by Abril and Iversen (2002). After creating the N₂ headspace, samples were vigorously shaken for 20 min and were placed in a thermostatic bath overnight at -1.6°C . The following day, the samples were shaken again for 20 min before starting the GC analysis. CH₄:CO₂:N₂ mixtures (Air Liquide, Belgium) of 1, 10 and 30 ppm CH₄ were used as standards. The concentrations were then computed using the CH₄ solubility coefficient given by Yamamoto et al. (1976). The accuracy of the measurements was within 1 %.

We calculated the solubility of CH₄ in seawater that is in equilibrium with the atmosphere, following Wiesenburg and Guinasso (1979). The ratio between the measured CH₄

concentration in seawater and the calculated solubility in equilibrated seawater determines the supersaturation factor.

2.3 CH₄ concentrations in bulk ice and brine

We used the wet extraction method to extract CH₄ from sea ice, as described in Raynaud et al. (1982) for continental ice. Briefly, 80 g of ice sample were put in a small container, using a 5 cm vertical resolution. The ice sample was then melted in the container under vacuum (10^{-3} torr), using a “bain-marie”. It was then slowly refrozen from the bottom, using an ethanol (96 %) bath that was cooled to -80°C by the addition of liquid N₂. After refreezing, the whole gas content (both dissolved and in the bubbles) was expelled into the headspace of the container. The expelled gas was then injected through a 22 mL packed column (Mole Sieve 5 A 80/100; 5 m \times 1/8”) into a gas chromatograph (Trace GC) equipped with a flame ionization detector for CH₄ measurement. The reproducibility of the measurement, based on triplicate analysis of five different standards, was 99.6 %.

The method described here above gives CH₄ concentrations in bulk ice. Providing that there is no CH₄ in the pure ice matrix (Weeks, 2010) and, hence, that the entire amount of CH₄ (dissolved or in gas bubbles) is found within the ice pores (i.e. brine channels), CH₄ concentration in bulk ice divided by the brine volume fraction (Cox and Weeks, 1983) gives the deduced CH₄ concentration in brine.

Dissolved CH₄ concentration in brine was also measured for brine samples collected using the sackhole technique (e.g. Gleitz et al., 1995; Papadimitriou et al., 2007). Sackholes (partial core holes) were drilled at different depths, ranging from 20 to 130 cm. Brines, from adjacent brine channels and pockets, seeped into the sackholes and were collected after 10 to 60 min using a peristaltic pump (Cole Palmer, Masterflex® – Environmental Sampler). Each sackhole remained covered with a plastic lid to minimize mixing with the free atmosphere. Brines were collected in 70 mL glass serum bottles, filled to overflowing, poisoned with 100 μL of saturated HgCl₂ and sealed with butyl stoppers and aluminium caps. The measured CH₄ concentration in brine is an integrated value of the CH₄ in brine from all the ice layers above the sampling depth. Therefore, the vertical resolution is lower than that of the CH₄ concentrations in brine that is deduced from the CH₄ concentrations in bulk ice. It is also noteworthy that the relative contribution of the various depth levels is unknown and dependent on the brine volume changes with depth. However, it is of interest to compare the measured CH₄ concentrations in brine with those deduced from the bulk ice values, as discussed later on.

For data interpretation, we calculated CH₄ solubility in brine and in ice (i.e. potential CH₄ concentration dissolved in brine and in bulk ice respectively). The solubility of CH₄ in brine was calculated using the same temperature and salinity-dependent solubility of Wiesenburg and Guinasso (1979) as for seawater. This is possible providing that the relationship

of Wiesenburg and Guinasso (1979) is valid for the ranges of brine temperature and brine salinity. As for the conversion of CH₄ concentrations in bulk ice into the deduced CH₄ concentrations in brine, we simply multiplied the solubility of CH₄ in brine by the brine volume fraction to get the solubility of CH₄ in bulk ice. Brine salinity and brine volume (used in the calculations) were derived from the relationship of Cox and Weeks (1983). The ratio between the observed CH₄ concentration in ice or brine to their respective calculated solubility determines the supersaturation factor.

In addition, we computed the standing stock of CH₄, i.e. the total amount of CH₄ within the ice cover. To do so, we integrated the concentrations of CH₄ in bulk ice vertically to obtain the CH₄ content per square metre of ice.

For further comparison with the literature, we also computed CH₄ mixing ratios. They are usually obtained by dividing the number of moles of CH₄ by the total gas content. However, since we did not measure the total gas content, we used the sum of measured atmospheric-dominant gases (O₂, N₂ and Ar; data not shown) instead.

3 Results

3.1 CH₄ concentrations in ice

CH₄ concentrations in bulk ice ranged from 3.4 nmol L_{ice}⁻¹ to 17.2 nmol L_{ice}⁻¹. Mean CH₄ concentration increased from BRW2 (6.4 nmol L_{ice}⁻¹) to BRW7 (7.8 nmol L_{ice}⁻¹) and decreased to 5.5 nmol L_{ice}⁻¹ at BRW10. This evolution parallels that of the standing stocks of CH₄, which increased from BRW2 (5070 to 5430 nmol m⁻²) to BRW7 (9200 nmol m⁻²), then decreased at BRW10 (7580 nmol m⁻²) (Fig. 2). For data interpretation, sea ice thickness is also shown in Fig. 2. It appears that the mean CH₄ concentration and the standing stock increased as sea ice thickened from BRW2 to BRW7, but decreased at BRW10 despite the fact that sea ice was thicker there.

The individual profiles of CH₄ concentrations in bulk ice (Fig. 3a) for each sampling event further highlight the contrasts between BRW10 and all the previous sampling events (BRW2 to BRW7): all the CH₄ concentration profiles in ice from BRW2 to BRW7 can be divided into three main zones. The first one ranged from 0 to 25 cm, where a peak of CH₄ concentration was found at 15 to 25 cm. CH₄ concentration measurements made on a twin ice core of BRW2 (duplicate) show that spatial variability in the 15 to 25 cm layer could reach 60 %. The second zone was found in the ice interior and ranged from 25 cm to the upper limit of the permeable layers (shaded area), where CH₄ concentrations were close to 5 nmol L_{ice}⁻¹. The third zone corresponds to the permeable layers where CH₄ concentration increased again toward the sea ice bottom, with values ranging from 5 to 10 nmol L_{ice}⁻¹. At BRW10, as the whole ice cover became permeable (shaded area at all depths), the whole profile flattened: the peak of

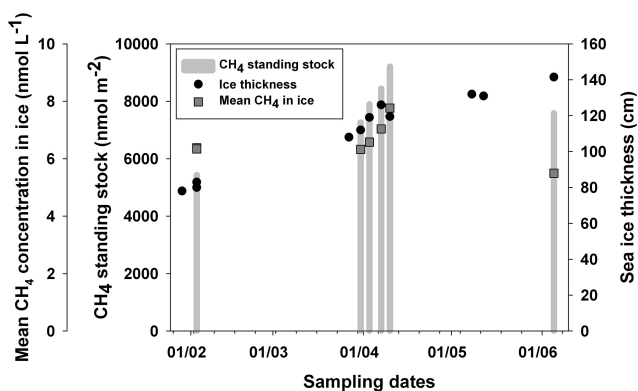


Figure 2. CH₄ standing stock for selected samplings events (vertical bars, from left to right, BRW2, BRW4, BRW5, BRW6, BRW7 and BRW10) in parallel with mean CH₄ concentration in sea ice and sea ice thickness.

CH₄ concentration around 15 to 25 cm disappeared, the ice interior still has a baseline at 5 nmol L_{ice}⁻¹ and the increase of CH₄ concentration at the bottom was less obvious than in the previous sampling events.

Beside the strong vertical variation, CH₄ concentrations in bulk ice were always higher than the solubility values in surface seawater that would have been in equilibrium with the atmosphere (3.8 nmol L_{sw}⁻¹) and the theoretical solubility in ice at all depths (Fig. 3a – white dots). CH₄ concentrations in bulk ice were on average 1.8 times higher than that in surface seawater and 75 times higher than the theoretical solubility in ice. The highest supersaturation factor reached 396 and was measured in BRW6, at a depth of 20 to 25 cm. Again, BRW10 differed from all the other sampling events, with a lower supersaturation factor (mean supersaturation and standard deviation were 11 ± 4 versus 86 ± 68 for BRW2 to BRW7).

The CH₄ mixing ratio (not shown) was also calculated for BRW2, BRW4, BRW7 and BRW10. It ranged from 5.8 to 105.3 ppmV. The maximum mixing ratio was found in BRW4, at a depth of 15 to 20 cm; this is 3.6 times higher than the mean mixing ratio of 29 ppmV.

To summarize, BRW10 differed from all the other samplings events by its lower mean CH₄ concentration and its flatter CH₄ concentration profiles. Although all the ice samples were supersaturated relative to surface seawater, larger supersaturations were observed from BRW2 to BRW7 (less permeable ice cores) compared to BRW10 (entirely permeable ice core), especially at a depth of 15 to 25 cm where both CH₄ concentrations and CH₄ mixing ratios were found to be the highest.

3.2 CH₄ concentrations in brine

Deduced CH₄ concentrations in brine (using CH₄ concentrations in ice) ranged from 13.2 nmol L_{brine}⁻¹ to

677.7 nmol L_{brine}⁻¹. These are thus much higher than the range of CH₄ concentrations measured in brine sackholes (10.0 to 36.2 nmol L_{brine}⁻¹) (Fig. 3 – triangles) and in seawater (25.9 and 116.4 nmol L_{sw}⁻¹).

The evolution of CH₄ concentrations in brine across seasons was rather similar to that of CH₄ concentrations in bulk ice, except in the bottom layers. Indeed, from BRW2 to BRW7, high CH₄ concentrations in brine were also observed at a depth of 15 to 20 cm; but from that level, CH₄ concentration in brine decreased and reached the lowest values at the sea ice bottom, where it is similar to observed CH₄ values in seawater. There was thus no increase of CH₄ concentration in brine at the sea ice bottom as observed in the CH₄ concentrations in bulk ice. The profile of CH₄ concentrations in brine flattened at BRW10, with values ranging between 13.2 and 87.0 nmol L_{brine}⁻¹, which were less variable and much closer to both the solubility values in brine and the actual measured CH₄ concentrations in brine than the ranges of values in the previous sampling events (35.6 nmol L_{brine}⁻¹ and 677.7 nmol L_{brine}⁻¹). The minimum CH₄ concentration in brine was calculated at 12.5 cm. Temperature data were missing at the very surface, so that we could not compute CH₄ concentrations in brine above 12.5 cm.

3.3 CH₄ concentrations in seawater

Measured CH₄ concentrations in seawater ranged from 25.9 to 116.4 nmol L_{sw}⁻¹ (Fig. 3c). This is 7 to 31 times higher than seawater in equilibrium with the atmosphere (3.8 nmol L⁻¹ for a salinity of 35 at 0 °C) (Wiesenburg and Guinasso, 1979).

Measurements of CH₄ concentrations in seawater were homogenous in time from BRW2 to BRW7, with a mean value and standard deviation of 42.0 ± 2.4 nmol L_{sw}⁻¹ for BRW2 and 37.5 ± 6 nmol L_{sw}⁻¹ for BRW4 to BRW7. They then increased at all depths at BRW10 and reached a mean value and standard deviation of 77.4 ± 27.8 nmol L_{sw}⁻¹.

4 Discussion

The present paper aims at understanding the physical controls on the CH₄ concentrations in sea ice. Discussing the physical controls only makes sense if the variations of CH₄ concentration due to biological activity are negligible compared to those due to physical processes. Therefore, we will first assess the importance of biological activity on the variation of CH₄ concentrations in sea ice and brine (Sect. 4.1) before discussing the physical controls (Sect. 4.2).

4.1 Impact of biological activity on CH₄ concentrations

To assess the impact of biological activity on CH₄ concentrations, we recalculated the standing stocks of BRW4 to BRW7 (Fig. 3), by considering every 5 cm ice sample in the 25 to 80 cm depth layers. These choices are motivated by the

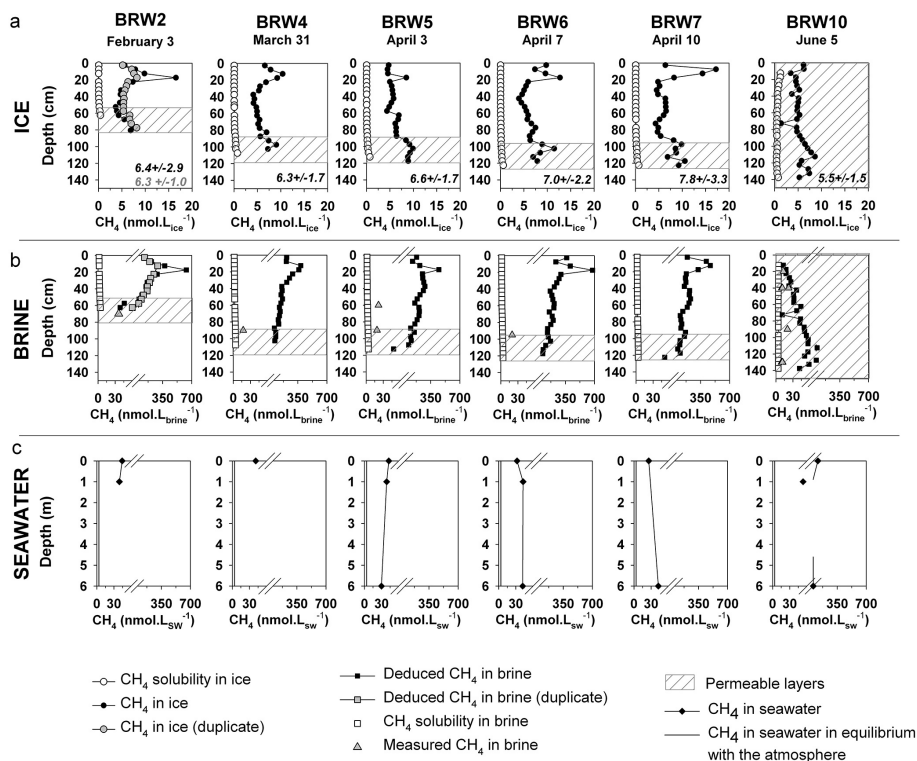


Figure 3. Evolution of CH₄ concentration in (a) bulk ice, (b) brine and (c) seawater (black dots, squares and diamonds respectively), compared to CH₄ solubility in ice, brine and seawater that is in equilibrium with the atmosphere (white dots, white squares and black straight lines respectively). Grey dots and grey squares are measurements made on duplicate samples of BRW2. Grey triangles in (b) are CH₄ measurements in brine sackholes. The break in the x axes of (b) and (c) is set at 60 nmol.L. Dashed areas are permeable layers (i.e. layers with a brine volume fraction above 5 %).

following reasons: first, we suggest focusing on the standing stocks of the impermeable layers (i.e. layers that have a brine volume fraction below 5 % (Golden et al., 1998); layers above the shaded areas on Fig. 3a, b). These layers are considered as a closed system in terms of brine dynamics and are therefore suitable for assessing biological transformation of CH₄. Second, we felt it appropriate to ignore the upper layer (0 to 25 cm), since spatial variability could be important in these layers (up to 60 % the 15 to 25 cm depth layer) as shown in Fig. 3a – BRW2. Third, we only focused on the sampling events that were collected at short time intervals (three or four days), i.e. BRW4 to BRW7 rather than BRW2 to BRW4 (56 days). This is mainly due to the similar physical properties of the ice cores collected at short time intervals (i.e. in terms of ice core length, ice temperature and ice salinity profiles).

Deduced CH₄ standing stocks in the 5 cm ice samples (in the 25 to 80 cm ice layer, from BRW4 to BRW7) varied between 198 and 375 nmol m⁻², with a mean and standard deviation of 271 ± 41 nmol m⁻². We performed an ANalysis Of VAriance (ANOVA) test on these standing stocks ($n = 44$) and differences between the samplings were not significant

enough to exclude the possibility of random sampling variability.

In addition, we plotted chlorophyll *a* concentrations against CH₄ concentrations in bulk ice and phosphate concentrations against CH₄ concentrations in bulk ice to investigate potential in situ production of CH₄ in both permeable and impermeable ice layers (see Appendix A). The rationale is that previous studies have shown a strong correlation between these variables (Damm et al., 2008, 2010) where CH₄ production was found to occur. As there is no obvious correlation between the presented variables (see Appendix A), we surmise that the pathway of CH₄ production that was observed in Damm et al. (2008, 2010) may not have occurred in the present study.

Furthermore, the turnover time for CH₄ oxidation in the Arctic Ocean exceeds 1.5 years (Griffiths et al., 1982, and Valentine et al., 2001), which is much longer than the lifetime of first-year landfast ice. If we assumed that the turnover time is similar in landfast sea ice, then we would not expect to find major CH₄ oxidation in our ice samples.

Because CH₄ production is unlikely in sea ice and CH₄ oxidation may be slow, we conclude that biological transformation of CH₄ is negligible in comparison with the amount of

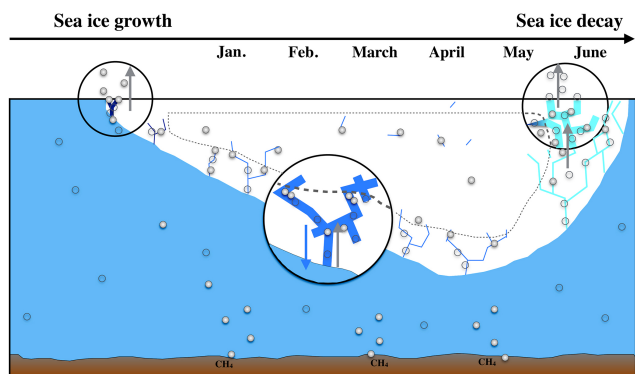


Figure 4. Schematic figure of CH_4 incorporation and release in sea ice. Sizes are intentionally disproportionate to highlight processes better. The area above the dotted line represents the impermeable layers. The small filled and empty circles represent CH_4 in gas bubbles and in dissolved state respectively. Upward grey arrows indicate the upward transport of gas bubbles due to their buoyancy, while downward blue arrows indicate the removal of dissolved gas through brine drainage. Large black circles zoom in on particular processes described in the text (Sect. 4.2): gas exchanges at the beginning of ice growth, gas accumulation predominantly under the impermeable layers and gas bubble escape during ice decay. Dark blue, light blue and cyan strokes in ice represent brine channels with high, moderate or low salinity respectively.

CH_4 that was physically incorporated in the impermeable ice layers; this is consistent with the findings derived from the standing stocks. Therefore, the discussion below will mainly focus on the physical processes that regulate CH_4 concentrations in sea ice.

4.2 Impact of physical processes on CH_4 concentrations

4.2.1 Range of CH_4 concentrations in sea ice and seawater, comparison with the literature

Our CH_4 concentrations in sea ice ($3.4\text{--}17.2\text{ nmol L}_{\text{ice}}^{-1}$) were slightly lower than those of Lorenson and Kvenvolden (1995) ($15\text{ to }40\text{ nmol L}_{\text{ice}}^{-1}$). The deduced mixing ratios ($5.8\text{ to }105.3\text{ ppmV}$) were, however, much lower than the $11\,000\text{ ppmV}$ of Shakhova et al. (2010). We attribute the observed differences to (1) the CH_4 concentrations in seawater and (2) ebullition processes (i.e. the seepage of CH_4 bubbles from the seafloor and their rising through the water column).

First, our CH_4 concentrations in seawater (25.9 and $116.4\text{ nmol L}_{\text{sw}}^{-1}$) are consistent with those reported in northern Alaska ($10.7\text{ to }111.8\text{ nmol L}_{\text{sw}}^{-1}$; Kvenvolden et al., 1993) and shallow shelf areas with CH_4 release from sediment and/or destabilized gas hydrate ($2.1\text{ to }154\text{ nmol L}_{\text{sw}}^{-1}$; Shakhova et al., 2005), but are much lower than the measurements reported by Shakhova et al. (2010) ($1.8\text{ to }2880\text{ nmol L}_{\text{sw}}^{-1}$). The differences in CH_4 concentrations in seawater lead to contrasting CH_4 supersaturations (700% and 3100% in the present study versus 100% to $160\,000\%$ in

Shakhova et al., 2010). Assuming similar incorporation rates in both studies, lower CH_4 supersaturation in seawater leads to lower CH_4 incorporated into sea ice and hence a lower CH_4 mixing ratio in sea ice.

Second, ebullition is a process associated with rapid bubble ascension, limiting gas equilibration with the surrounding water mass (Keller and Stallard, 1994). Therefore, in shallow locations, CH_4 bubbles released from the seafloor could reach the seawater surface (Keller and Stallard, 1994; McGinnis et al., 2006). We believe that ebullition could increase CH_4 at the sea-ice–water interface and lead to larger CH_4 incorporation into sea ice than if the ebullition was absent. Ebullitions were clearly observed in the Siberian Arctic Shelf (Shakhova et al., 2010) and, in that particular case, centimetre-sized bubbles were found within the ice (Shakhova et al., 2010). Since we did not find any literature reporting ebullition processes at Barrow and since our ice cores generally showed millimetre-sized bubbles (Zhou et al., 2013), we believe that ebullition processes were much less important in our study than in Shakhova et al. (2010).

4.2.2 Mechanisms responsible for the evolution of the vertical profiles of CH_4 concentrations in bulk ice and brine during ice growth

Although the CH_4 source was seawater, CH_4 concentrations in bulk ice from BRW2 to BRW7 did not show a C-shaped profile, as would salinity for growing sea ice (Petrich and Eicken, 2010). For instance, instead of a surface maximum for salt, we observed a subsurface maximum for CH_4 . As discussed below, we propose three abiotic mechanisms to explain the salient features of the vertical profiles of CH_4 concentration in Barrow bulk ice: (1) gas escape during the initial ice growth phase in the surface layer, (2) predominant gas accumulation in the subsurface and (3) brine volume fraction effect for the bottom layer.

We assume that CH_4 , similarly to CO_2 , could escape from the ice to the atmosphere at the beginning of the ice growth (Geilfus et al., 2013; Nomura et al., 2006) (Fig. 4). In addition, once sea ice is consolidated, changes in temperature and in the volume of brine pockets are likely to fracture the ice, causing the expulsion of brines (Notz and Worster, 2009) and air bubbles (Untersteiner, 1968) at the ice surface. These two processes could explain the decrease of CH_4 concentrations in bulk ice right at the surface of sea ice (Fig. 3).

Predominant gas accumulation during ice growth has been described for argon (Ar) in Zhou et al. (2013): in addition to brine concentration, temperature and salinity changes in brine at sea ice formation lead to a sharp decrease of CH_4 solubility that favours bubble nucleation in sea ice. Once formed, the bubbles migrate upward due to their buoyancy. They are trapped under the impermeable surface layer, leading to gas accumulation (Fig. 4). Such a process is supported by two characteristics: the presence of bubbles and the occurrence of large supersaturation levels (compared to the rest of

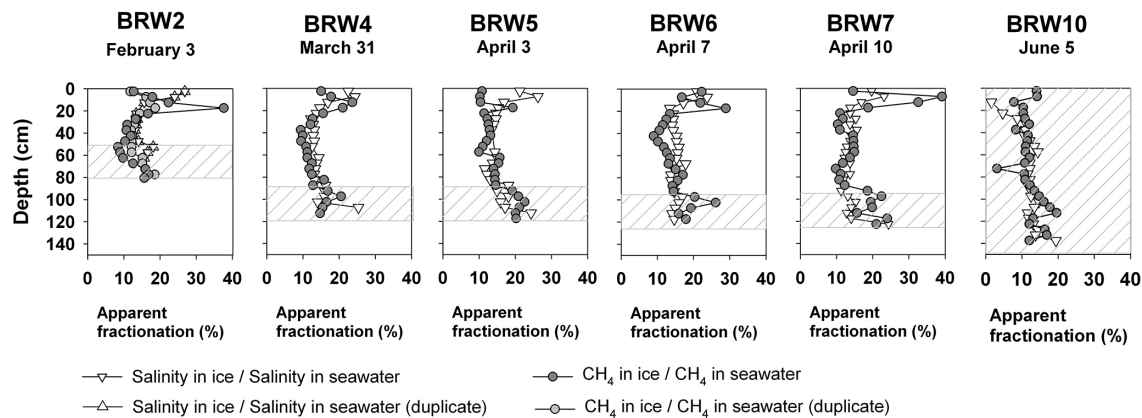


Figure 5. Comparison between the apparent fractionation of salinity in ice (the ratio between ice salinity and seawater salinity (32)) and the apparent fractionation of CH₄ (the ratio between CH₄ in ice and CH₄ in seawater (44 nmol L_{sw}⁻¹)). The seawater salinity and CH₄ in seawater that are chosen as references were the values obtained from BRW2. Dashed areas are permeable layers (i.e. layers with a brine volume fraction above 5 %).

the ice core). The presence of bubbles was observed in thin sections by Zhou et al. (2013) and is also consistent with the large difference between the deduced CH₄ in brine (which includes both CH₄ in bubbles and CH₄ that is dissolved in brine) (Fig. 3b, squares) and the actual measurements of CH₄ in brine (only CH₄ that is dissolved in brine) (Fig. 3, triangles). Moreover, the largest CH₄ supersaturations relative to CH₄ solubility in ice were always found at a depth of 15 to 25 cm, which corresponds to the ice depth where Zhou et al. (2013) have observed bubble accumulation and Ar supersaturation up to 2900 %. Therefore, the mechanism of predominant gas accumulation suggested for Ar may be relevant for CH₄ as well. Larger CH₄ supersaturation as compared to Ar supersaturation is likely due to the difference in CH₄ and Ar solubility; CH₄, which is less soluble than Ar, would be more affected by temperature and salinity changes. It is also noteworthy that this process of bubble formation in sea ice led to large spatial variability as witnessed by the duplicate of BRW2, which showed up to 60 % of CH₄ variation at a depth of 15 to 25 cm.

As the freezing front progresses, the temperature gradient in the permeable layer reduces; bubble nucleation due to solubility decrease is less efficient. As a consequence, CH₄ accumulates less and CH₄ concentration in brine decreases towards the bottom. Such a decrease is however not observed for CH₄ concentration in bulk ice. We attribute this to the brine volume fraction effect: a larger brine volume may contain a larger amount of CH₄ molecules, which induces higher CH₄ concentrations in bulk ice. The fact that CH₄ in brine did not show an increase at the bottom of the ice supports this suggestion.

An alternative explanation for the predominant gas accumulation due to solubility changes would be that of a direct bubble incorporation after a sudden but intense release of CH₄ bubbles from the sediment to the ice bottom. CH₄

release from sediment is possible since our CH₄ concentrations in seawater are consistent with those found in areas where CH₄ release from sediment and/or gas hydrate destabilization likely occurs (see Sect. 4.2.1). However, this process does not explain the slow decrease of CH₄ concentration in brine from a depth of 15 to 25 cm to the sea ice bottom (Fig. 3b), and we may also wonder why the ebullition only occurred once during the whole sampling period.

The contribution of in situ bubble formation in the retention of CH₄ in sea ice is assessed in Fig. 5. We calculated the ratio between CH₄ in ice and the CH₄ in seawater at BRW2 (44 nmol L_{sw}⁻¹) and the ratio between brine salinity and the salinity of seawater at BRW2 (32) at each ice depth for all the sampling events. The CH₄ in seawater and the salinity of seawater of BRW2 were chosen as references for the sake of consistency with Zhou et al. (2013). Similar apparent fractionation means that CH₄ is retained (incorporated and transported) in sea ice in the same way to salt, while a difference in the apparent fractionation means a difference in their retention processes.

Four main observations can be made with regard to Fig. 5. First, the apparent fractionation averaged 15 % but never reached 100 %. This is due to the rejection of impurities during sea ice formation (Weeks, 2010). Our study therefore suggests that sea ice rejects about 85 % of its impurities, but retains 15 % of them. This is in agreement with Petrich and Eicken (2010), who suggested that sea ice brine allows a retention of 10 to 40 % of seawater ions in the ice. Second, the highest apparent fractionation of CH₄ (up to 39 %) was observed at a depth of 15 to 25 cm; in that layer, the retention of CH₄ could be higher than that of salt by a factor of 2. This supports the previous suggestion about predominant gas accumulation: the presence of gas bubbles allows higher retention of CH₄ than salt. Third, the apparent fractionation of CH₄ was lower than that of salt at the surface

of all the sampling events, except at BRW10. That lower apparent fractionation may be related to the large permeability of the ice during its formation and/or the formation of some cracks at the ice surface (during the cold period), which have allowed gas to escape from sea ice to the atmosphere, as explained earlier in this section. The lower CH₄ concentrations in bulk ice at these sampling events (Fig. 3a) tends to support the conjecture of gas escape. Fourth, below the top layer of about 25 cm of ice, both CH₄ and salt enrichment values are similar, indicating that, in these ice layers, CH₄ was mainly incorporated in the dissolved state in the same way as salt.

4.2.3 Sea ice permeability controls CH₄ concentrations in bulk ice and brine during sea ice decay

At BRW10, both CH₄ concentrations in bulk ice and deduced CH₄ concentrations in brine decreased and became less variable than the previous samplings (BRW2 to BRW7). In addition, CH₄ standing stocks decreased by ca. 1600 nmol m⁻² from BRW7 to BRW10, and the deduced CH₄ concentrations in brine approached the measured concentrations. These measurements suggest that there is an enhanced gas transport through the ice and that gas bubbles have escaped from sea ice to the atmosphere. Gas escape was possible given that sea ice was permeable at all depths (Fig. 3a, b, shaded area). Concomitant Ar bubble escape was suggested in Zhou et al. (2013). However, in contrast to Ar that was then at saturation, CH₄ was still supersaturated compared to the solubility in brine. This could be related to a slow exchange between the atmosphere, brine and the supersaturated seawater through diffusion.

CH₄ concentrations in brine at BRW10 (13.2 to 87.0 nmol L_{brine}⁻¹) were lower than the CH₄ concentration at the ice/water interface (116.4 nmol L_{sw}⁻¹), but higher than the theoretical CH₄ solubility in surface seawater that is in equilibrium with the atmosphere (3.8 nmol L_{sw}⁻¹). Although the CH₄ concentrations in brine right at the surface (0–12.5 cm) could not be retrieved, we can hypothesize that the gradient of CH₄ concentrations between the ice/seawater interface and the ice surface led to CH₄ diffusion from the ice/seawater interface to the ice surface and therefore maintained CH₄ supersaturation in ice after gas bubble escape. Since the source of CH₄ came from supersaturated seawater, CH₄ concentrations in brine were slightly higher at the sea ice bottom than at the top.

5 Conclusions and perspectives

We reported on the evolution of CH₄ concentrations in landfast sea ice, brine and under-ice water from February through June 2009 at Barrow (Alaska). Our CH₄ concentrations in sea ice in seawater are consistent with records from the area with CH₄ release from sediment and gas

hydrate destabilization (Kvenvolden et al., 1993; Lorenson and Kvenvolden, 1995; Shakhova et al., 2010).

We suggest that brine concentration and strong solubility decrease triggered gas bubble formation, which favoured CH₄ accumulation in ice. As a result, CH₄ retention in the ice was twice as efficient as that of salt. However, as summarized in Fig. 4, gas exchange likely took place during initial ice growth between sea ice and the atmosphere, and the formation of cracks could also lead to a decrease of CH₄ right at the surface of the ice. Also, as sea ice thickened, temperature and brine salinity gradient were no longer sufficient to trigger bubble nucleation, and CH₄ was then trapped in the dissolved state in the same way as salt. The subsequent evolution of CH₄ concentrations in sea ice layers mainly depended on physical processes, as chlorophyll *a* and phosphate concentrations did not support in situ CH₄ production and as CH₄ oxidation was likely insignificant. Abrupt changes in CH₄ concentrations in sea ice occurred when sea ice became permeable; these were associated with the release of gas bubbles to the atmosphere. Therefore, the main role of our landfast sea ice in the exchange of CH₄ from seawater to the atmosphere was its control of the amount of CH₄ that it is able to store in its impermeable layers and the duration of such storage.

Although gas incorporation and sea ice permeability were two dominant factors driving CH₄ concentrations in sea ice in our study site, the magnitude of these processes may be different in other polar seas. Indeed, the contribution of the ebullition fluxes of CH₄ from sediment to the concentration of CH₄ in bulk ice, the transport of CH₄ through the ice and the significance of physical and biological controls on CH₄ dynamics rely on the nature of the sediment, the water depth, the physical parameters of the ice and biological activity within the ice, which may vary depending on the location.

In the case of a higher mix of physical and biological controls on CH₄ concentrations in bulk ice, we would recommend measuring: (1) the carbon and hydrogen isotopes of CH₄ in sea ice, as isotopic fractionation is highly sensitive to biological processes; and (2) the same isotopes in the sources (e.g. organic matter). Indeed, previous studies have suggested that the carbon isotopic values of biogenic CH₄ within anoxic sediments may be as negative as -110‰ (Whiticar, 1999) in comparison to those resulting from CH₄ oxidation (-10 to -24‰; Damm et al., 2008; Schubert et al., 2011), but few of them have considered that the measured isotopic values in the sediment or in seawater also depend on the isotopic composition of the sources.

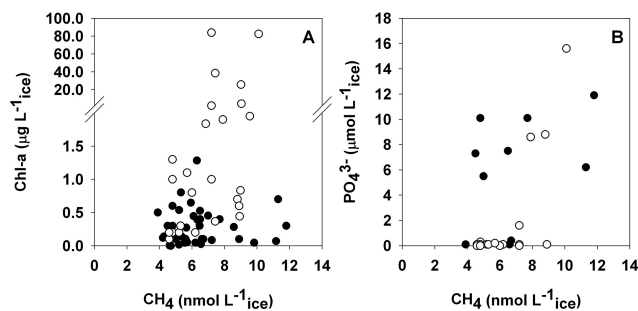
Appendix A: Relationships between chlorophyll *a* and CH₄ concentrations and between phosphate and CH₄ concentrations in sea ice

Figure A1. Relationships between (A) chlorophyll *a* (Chl *a*) and methane (CH₄) concentrations, and (B) phosphate (PO₄³⁻) and CH₄ concentrations in sea ice. Open and closed circles indicate respectively permeable and impermeable ice layers (i.e. a brine volume fraction above or below 5%). Chl *a* and PO₄³⁻ data are from Zhou et al. (2013); Chl *a* data were available for all the sampling events that are presented here, while PO₄³⁻ data were only available for BRW2, BRW7 and BRW10.

Acknowledgements. The authors would like to thank Hajo Eicken, the rest of the sea ice group of the Geophysical Institute of the University of Alaska Fairbanks, Tim Papakyriakou, Bernard Heinesch, Michel Yernaux, Frédéric Brabant, Thomas Goossens, Noémie Carnat and Rodd Laing for their help during fieldwork. We are indebted to the Barrow Arctic Science Consortium and the North Slope Borough for their logistical support. We also thank Saïda El Amri and Arnaud Rottier for their efficient help with laboratory work, Ceri Middleton for language help and Célia Sapart and Neige Egmont for their comments. Our gratitude also goes to the three anonymous reviewers as their comments have greatly improved the quality of the manuscript. This research was supported by the F.R.S-FNRS (contract 2.4584.09), the National Science Foundation (project OPP-0632398 (SIZONet)), the University of Alaska Fairbanks and the Belgian Science Policy (contract SD/CA/03A), the NCE ArcticNet and National Science and Engineering Research Council (NSERC). N.-X. Geilfus received a PhD grant from F.R.S.-FRIA and acknowledges the Canada Excellence Research Chair Program and the Arctic Science Partnership (ASP). J. Zhou is a research fellow of F.R.S.-FNRS, and B. Delille is a research associate of F.R.S.-FNRS. This is MARE contribution no. 265.

Edited by: L. Kaleschke

References

- Abril, G. and Iversen, N.: Methane dynamics in a shallow non-tidal estuary (Randers Fjord, Denmark), *Mar. Ecol.-Prog. Ser.*, 230, 171–181, 2002.
- Bange, H. W., Bartell, U. H., Rapsomanikis, S., and Andreae, M. O.: Methane in the Baltic and North Seas and a Reassessment of the Marine Emissions of Methane, *Global Biogeochem. Cy.*, 8, 465–480, 1994.
- Bates, T. S., Kelly, K. C., Johnson, J. E., and Gammon, R. H.: A reevaluation of the open ocean source of methane to the atmosphere, *J. Geophys. Res.*, 101, 6953–6961, 1996.
- Borges, A. V. and Abril, G.: 5.04 – Carbon Dioxide and Methane Dynamics in Estuaries, in: *Treatise on Estuarine and Coastal Science*, Editors-in-Chief: Eric, W. and Donald, M. (Eds.), Academic Press, Waltham, 2011.
- Cox, G. F. N. and Weeks, W. F.: Equations for determining the gas and brine volumes in sea-ice samples, *J. Glaciol.*, 29, 306–316, 1983.
- Damm, E., Schauer, U., Rudels, B., and Haas, C.: Excess of bottom-released methane in an Arctic shelf sea polynya in winter, *Cont. Shelf Res.*, 27, 1692–1701, 2007.
- Damm, E., Kiene, R. P., Schwarz, J., Falck, E., and Dieckmann, G.: Methane cycling in Arctic shelf water and its relationship with phytoplankton biomass and DMSP, *Mar. Chem.*, 109, 45–59, 2008.
- Damm, E., Helmke, E., Thoms, S., Schauer, U., Nöthig, E., Bakker, K., and Kiene, R. P.: Methane production in aerobic oligotrophic surface water in the central Arctic Ocean, *Biogeosciences*, 7, 1099–1108, doi:10.5194/bg-7-1099-2010, 2010.
- Florez-Leiva, L., Damm, E., and Fariñas, L.: Methane production induced by dimethylsulfide in surface water of an upwelling ecosystem, *Prog. Oceanogr.*, 112–113, 38–48, doi:10.1016/j.pocean.2013.03.005, 2013.
- Geilfus, N. X., Carnat, G., Papakyriakou, T., Tison, J. L., Else, B., Thomas, H., Shadwick, E., and Delille, B.: Dynamics of $p\text{CO}_2$ and related air-ice CO_2 fluxes in the Arctic coastal zone (Amundsen Gulf, Beaufort Sea), *J. Geophys. Res.-Oceans*, 117, C00G10, doi:10.1029/2011JC007118, 2012.
- Geilfus, N. X., Carnat, G., Dieckmann, G. S., Halden, N., Nehrke, G., Papakyriakou, T., Tison, J. L., and Delille, B.: First estimates of the contribution of CaCO_3 precipitation to the release of CO_2 to the atmosphere during young sea ice growth, *J. Geophys. Res.-Oceans*, 118, 244–255, 2013.
- Gleitz, M., v. d. Loeff, M. R., Thomas, D. N., Dieckmann, G. S., and Millero, F. J.: Comparison of summer and winter in organic carbon, oxygen and nutrient concentrations in Antarctic sea ice brine, *Mar. Chem.*, 51, 81–91, 1995.
- Golden, K. M., Ackley, S. F., and Lytle, V. I.: The percolation phase transition in sea ice, *Science*, 282, 2238–2241, 1998.
- Griffiths, R. P., Caldwell, B. A., Cline, J. D., Broich, W. A., and Morita, R. Y.: Field observations of methane concentrations and oxidation rates in the southeastern Bering Sea, *Appl. Environ. Microb.*, 44, 435–446, 1982.
- He, X., Sun, L., Xie, Z., Huang, W., Long, N., Li, Z., and Xing, G.: Sea ice in the Arctic Ocean: Role of shielding and consumption of methane, *Atmos. Environ.*, 67, 8–13, 2013.
- Judd, A. G.: Natural seabed gas seeps as sources of atmospheric methane, *Environ. Geol.*, 46, 988–996, 2004.
- Karl, D. M., Beversdorf, L., Bjorkman, K. M., Church, M. J., Martinez, A., and DeLong, E. F.: Aerobic production of methane in the sea, *Nat. Geosci.*, 1, 473–478, 2008.
- Keller, M. and Stallard, R. F.: Methane emission by bubbling from Gatun Lake, Panama, *J. Geophys. Res.*, 99, 8307–8319, 1994.
- Kirschke, S., Bousquet, P., Ciais, P., Saunoy, M., Canadell, J. G., Dlugokencky, E. J., Bergamaschi, P., Bergmann, D., Blake, D. R., Bruhwiler, L., Cameron-Smith, P., Castaldi, S., Chevallier, F., Feng, L., Fraser, A., Heimann, M., Hodson, E. L., Houweling, S., Josse, B., Fraser, P. J., Krummel, P. B., Lamarque, J.-F., Langenfelds, R. L., Le Quere, C., Naik, V., O'Doherty, S., Palmer, P. I., Pison, I., Plummer, D., Poulter, B., Prinn, R. G., Rigby, M., Ringeval, B., Santini, M., Schmidt, M., Shindell, D. T., Simpson, I. J., Spahni, R., Steele, L. P., Strode, S. A., Sudo, K., Szopa, S., van der Werf, G. R., Voulgarakis, A., van Weele, M., Weiss, R. F., Williams, J. E., and Zeng, G.: Three decades of global methane sources and sinks, *Nat. Geosci.*, 6, 813–823, 2013.
- Kitidis, V., Upstill-Goddard, R. C., and Anderson, L. G.: Methane and nitrous oxide in surface water along the North-West Passage, Arctic Ocean, *Mar. Chem.*, 121, 80–86, 2010.
- Kort, E. A., Wofsy, S. C., Daube, B. C., Diao, M., Elkins, J. W., Gao, R. S., Hints, E. J., Hurst, D. F., Jimenez, R., Moore, F. L., Spackman, J. R., and Zondlo, M. A.: Atmospheric observations of Arctic Ocean methane emissions up to 82[deg] north, *Nat. Geosci.*, 5, 318–321, 2012.
- Kvenvolden, K., Lilley, M. D., and Lorenson, T. D.: The Beaufort Sea Continental Shelf as a seasonal source of atmospheric methane, *Geophys. Res. Lett.*, 20, 2459–2462, 1993.
- Lawrence, D. M., Slater, A. G., Tomas, R. A., Holland, M. M., and Deser, C.: Accelerated Arctic land warming and permafrost degradation during rapid sea ice loss, *Geophys. Res. Lett.*, 35, L11506, doi:10.1029/2008gl033985, 2008.
- Loose, B., McGillis, W. R., Schlosser, P., Perovich, D., and Takahashi, T.: Effects of freezing, growth, and ice cover on gas trans-

- port processes in laboratory seawater experiments, *Geophys. Res. Lett.*, 36, L05603, doi:10.1029/2008gl036318, 2009.
- Lorenson, T. D. and Kvenvolden, K. A.: Methane in coastal seawater, sea ice and bottom sediments, Beaufort Sea, Alaska: U.S. Geological Survey Open-File Report 95-70, US Geological Survey, Menlo Park, CA, 1995.
- McGinnis, D. F., Greinert, J., Artemov, Y., Beaubien, S. E., and Wüest, A.: Fate of rising methane bubbles in stratified waters: How much methane reaches the atmosphere?, *J. Geophys. Res.*, 111, C09007, doi:10.1029/2005jc003183, 2006.
- Myhre, G., D. Shindell, F.-M. Bréon, W. Collins, J. Fuglestedt, J. Huang, D. Koch, J.-F. Lamarque, D. Lee, B. Mendoza, T. Nakajima, A. Robock, G. Stephens, T. Takemura, and Zhang, H.: *Anthropogenic and Natural Radiative Forcing*, Cambridge University Press, Cambridge, United Kingdom and New York, NY, USA, 2013.
- Nomura, D., Yoshikawa-Inoue, H., and Toyota, T.: The effect of sea-ice growth on air-sea CO₂ flux in a tank experiment, *Tellus B*, 58, 418–426, 2006.
- Nomura, D., Eicken, H., Gradinger, R., and Shirasawa, K.: Rapid Physically driven invasion of the air-sea ice CO₂ flux in the seasonal landfast ice off Barrow, Alaska after onset of surface melt, *Cont. Shelf Res.*, 30, 1998–2004, 2010.
- Notz, D. and Worster, M. G.: Desalination processes of sea ice revisited, *J. Geophys. Res.*, 114, C05006, doi:10.1029/2008JC004885, 2009.
- O'Connor, F. M., Boucher, O., Gedney, N., Jones, C. D., Folberth, G. A., Coppel, R., Friedlingstein, P., Collins, W. J., Chappellaz, J., Ridley, J., and Johnson, C. E.: Possible role of wetlands, permafrost, and methane hydrates in the methane cycle under future climate change: A review, *Rev. Geophys.*, 48, RG4005, doi:10.1029/2010RG000326, 2010.
- Papadimitriou, S., Thomas, D. N., Kennedy, H., Haas, C., Kuosa, H., Krell, A., and Dieckmann, G. S.: Biogeochemical composition of natural sea ice brines from the Weddell Sea during early austral summer, *Limnol. Oceanogr.*, 52, 1809–1823, 2007.
- Petrich, C. and Eicken, H.: Growth, Structure and Properties of Sea Ice, in: *Sea ice*, edited by: Thomas, D. N. and Dieckmann, G. S., Blackwell Publishing Ltd, UK, 2010.
- Raynaud, D., Delmas, R., Ascencio, J. M., and Legrand, M.: Gas extraction from polar ice cores: a critical issue for studying the evolution of atmospheric CO₂ and ice-sheet surface elevation, *Ann. Glaciol.*, 3, 265–268, 1982.
- Reagan, M. T. and Moridis, G. T.: Dynamic response of oceanic hydrate deposits to ocean temperature change, *J. Geophys. Res.*, 113, C12023, doi:10.1029/2008JC004938, 2008.
- Romanovskii, N. N., Hubberten, H. W., Gavrillov, A. V., Tumskey, V. E., Tipenko, G. S., Grigoriev, M. N., and Siegert, C.: Thermokarst and land-ocean interactions, Laptev Sea Region, Russia, *Permafrost Periglac.*, 11, 137–152, 2000.
- Savichev, A. S., Rusanov, I. I., Yusupov, S. K., Pimenov, N. V., Lein, A. Y., and Ivanov, M. V.: The biogeochemical cycle of methane in the coastal zone and littoral of the Kandalaksha Bay of the White Sea, *Microbiology+*, 73, 457–468, 2004.
- Schubert, C. J., Vazquez, F., Lösekann-Behrens, T., Knittel, K., Tonolla, M., and Boetius, A.: Evidence for anaerobic oxidation of methane in sediments of a freshwater system (Lago di Cadagno), *FEMS Microbiol. Ecol.*, 76, 26–38, 2011.
- Shakhova, N., Semiletov, I., and Panteleev, G.: The distribution of methane on the Siberian Arctic shelves: Implications for the marine methane cycle, *Geophys. Res. Lett.*, 32, L09601, doi:10.1029/2005GL022751, 2005.
- Shakhova, N., Semiletov, I., Salyuk, A., Yusupov, V., Kosmach, D., and Gustafsson, O.: Extensive Methane Venting to the Atmosphere from Sediments of the East Siberian Arctic Shelf, *Science*, 327, 1246–1250, 2010.
- Skoog, D. A., West, D. M., and Holler, F. J.: *Chimie analytique*, De Boeck Université, Paris, Bruxelles, 1997.
- Untersteiner, N.: Natural desalination and equilibrium salinity profile of perennial sea ice, *J. Geophys. Res.*, 73, 1251–1257, 1968.
- Upstill-Goddard, R. C., Barnes, J., Frost, T., Punshon, S., and Owens, N. J. P.: Methane in the southern North Sea: Low-salinity inputs, estuarine removal, and atmospheric flux, *Global Biogeochem. Cy.*, 14, 1205–1217, 2000.
- Weeks, W. F.: *On sea ice*, University of Alaska Press, Fairbanks, Alaska, 2010.
- Westbrook, G. K., Thatcher, K. E., Rohling, E. J., Piotrowski, A. M., Pälike, H., Osborne, A. H., Nisbet, E. G., Minshull, T. A., Lanoisellé, M., James, R. H., Hühnerbach, V., Green, D., Fisher, R. E., Crocker, A. J., Chabert, A., Bolton, C., Beszczynska-Möller, A., Berndt, C., and Aquilina, A.: Escape of methane gas from the seabed along the West Spitsbergen continental margin, *Geophys. Res. Lett.*, 36, L15608, doi:10.1029/2009GL039191, 2009.
- Whiticar, M. J.: Carbon and hydrogen isotope systematics of bacterial formation and oxidation of methane, *Chem. Geol.*, 161, 291–314, 1999.
- Wiesenburg, D. A. and Guinasso, N. L.: Equilibrium solubilities of methane, carbon monoxide and hydrogen in water and sea water, *J. Chem. Eng. Data*, 24, 356–360, 1979.
- Yamamoto, S., Alcauskas, J. B., and Crozier, T. E.: Solubility of methane in distilled water and seawater, *J. Chem. Eng. Data*, 21, 78–80, 1976.
- Zeikus, J. G. and Winfrey, M. R.: Temperature limitation of methanogenesis in aquatic sediments, *Appl. Environ. Microb.*, 31, 99–107, 1976.
- Zhou, J., Delille, B., Eicken, H., Vancoppenolle, M., Brabant, F., Carnat, G., Geilfus, N.-X., Papakyriakou, T., Heinesch, B., and Tison, J.-L.: Physical and biogeochemical properties in landfast sea ice (Barrow, Alaska): Insights on brine and gas dynamics across seasons, *J. Geophys. Res.-Ocean*, 118, 3172–3189, 2013.
- Zindler, C., Bracher, A., Marandino, C. A., Taylor, B., Torrecilla, E., Kock, A., and Bange, H. W.: Sulphur compounds, methane, and phytoplankton: interactions along a north-south transit in the western Pacific Ocean, *Biogeosciences*, 10, 3297–3311, doi:10.5194/bg-10-3297-2013, 2013.